

Influence of Aerosil-200 Nanofiller on the Flexural and Compressive Behaviour of Glass Fiber Reinforced Epoxy Composites

C Venkateshwar Reddy¹, G Ashwin Prabhu^{2}, A Kalyan Charan³, Vijaykumar B P⁴, Vishwa P⁵, and Tanveer Ahmed S⁶*

¹Assistant Professor, Department of Mechanical Engineering, Matrusri Engineering College, Saidabad, Hyderabad - 500059, India

²Assistant Professor, Department of Mechanical Engineering, St. Joseph's College of Engineering, Old Mahabalipuram Road, Chennai – 600119, Tamil Nadu, India

³Assistant Professor, Department of Mechanical Engineering, Matrusri Engineering College, Saidabad, Hyderabad - 500059, India

⁴Assistant professor, Department of Mechanical engineering, Ballari Institute of Technology and Management, Ballari, affiliated to Visvesvaraya Technological University, Belagavi, Karnataka 583104, India

⁵UG Scholar, Department of Mechanical Engineering, St. Joseph's College of Engineering, Old Mahabalipuram Road, Chennai – 600119, Tamil Nadu, India

⁶UG Scholar, Department of Mechanical Engineering, St. Joseph's College of Engineering, Old Mahabalipuram Road, Chennai – 600119, Tamil Nadu, India

Abstract. This study examines the impact of Aerosil-200 nanofiller on the mechanical properties of glass fiber reinforced epoxy composites in laminated plates and thin cylindrical shells. Composite specimens were produced with a hand lay-up method with nanofiller contents of 0%, 1%, 2%, 3%, and 4% by weight. Flexural tests on laminated specimens (ASTM D790) and compression tests on cylindrical shells were conducted to assess the impact of nanofiller on bending resistance and axial load-bearing capacity. The experimental results demonstrate a gradual improvement in flexural strength with an increase in nanofiller content up to 3%, with a maximum strength of 590.59 N/mm², in contrast to 399.9 N/mm² for the unfilled laminate. A comparable trend is noted in compression testing, wherein the 3% nanofiller shell demonstrates the maximum compressive strength of 157.663 N/mm² and a peak load of 58.230 kN. The 4% filled sample exhibits diminished performance, with strength decreasing to 116.34 N/mm². The results indicate that Aerosil-200 markedly improves mechanical performance up to an ideal filler concentration of 3%, after which material degradation ensues. This study offers critical insights for optimizing nanofiller loading in composite materials to enhance flexural and compressive performance.

* Corresponding author: ashwin.prabhu1990@gmail.com

1. Introduction

Composite materials have revolutionized engineering and production by providing new property combinations that traditional materials cannot achieve. These materials are synthesized by amalgamating two or more constituents at a macroscopic scale, such as glass fibers and epoxy resin. The reinforcing phase provides strength and rigidity, whereas the matrix phase anchors the reinforcement and enables stress transfer among fibers. Composites can be tailored to attain particular attributes, such as a high strength-to-weight ratio, corrosion resistance, or electrical conductivity. Their adaptability renders them essential in sectors including aerospace, automobile, construction, and sports equipment. A comprehensive understanding of composite behaviour is crucial for improving performance and developing materials with enhanced properties. Kadam et al. [1] demonstrated that the buckling behaviour of slender composite cylinders is significantly influenced by geometry, thermal stresses, and defects. Omidi et al. [2] underscored the impact of cuts and flaws on load-bearing capacity, whereas Godwin et al. [3] illustrated the essential importance of material and geometric characteristics in establishing the buckling factors in composite cylinders. The addition of fillers, including Al_2O_3 , clay, and carbon nanotubes, has demonstrated an enhancement in mechanical properties; for instance, Mohan Prasad et al. [4] observed increased hardness and tensile strength in hybrid glass/epoxy nanocomposites. Diwakar et al. [5] and Narayana et al. [6] emphasized the importance of stacking angle, shell thickness, and fiber orientation in enhancing axial load-bearing capability. Wagner et al. [7] executed a comprehensive computational and experimental study demonstrating the influence of defects on knockdown factors in composite cylinders.

Researchers have investigated the crashworthiness and energy-absorption properties of composite tubular constructions. Rabiee and Ghasemnejad [8] examined the advanced crushing mechanisms in polymer matrix tubes, highlighting the significance of nano-scale fillers in improving crush resistance. Abd El Baky et al. [9] established that hybrid glass/jute composites encasing aluminum tubes exhibit superior structural performance for automotive applications. Nagaraja et al. [10] demonstrated that hybridization enhances interfacial bonding and mechanical strength in polymer composites. The impact resistance of curved laminates was examined by Harris et al. [11], demonstrating that curvature and laminate thickness significantly influence structural performance. Research concentrating on the flexural behaviour of GFRP laminates has demonstrated that the incorporation of fillers markedly influences bending stiffness and failure mechanisms. Zhang et al. [12] assessed pultruded GFRP bridge deck laminates and determined that filler-modified matrices enhance bending performance. Hara et al. [13] investigated U-shaped composite springs and documented enhancements in flexural rigidity. Cheloni et al. [14] evaluated bending analysis techniques for fiberglass/epoxy laminates, determining that the incorporation of fillers improves load-bearing capacity and diminishes deflection during three-point bending.

The incorporation of nanoparticles is noteworthy due to their capacity to modify the resin microstructure and impede polymer chain mobility. Fumed silica, nano clay, graphene, and carbon nanotubes have been thoroughly studied to enhance the mechanical properties of GFRP systems. Singh et al. [15] established that silica nanoparticles augment stiffness and boost interlaminar shear strength in epoxy composites. Kumar et al. [16] discovered that graphene nanoplatelets enhance both flexural and compressive strength. Ramesh et al. [17] and Patel et al. [18] similarly documented significant enhancements in mechanical and fracture properties by the utilization of fumed silica-based nanofillers. Musa et al. [19] investigated nano clay-reinforced GFRP laminates and noted enhancements in flexural modulus and crack resistance. Akram et al. [20] demonstrated that nano clay - SiO_2 improves impact strength and diminishes micro-void development inside the matrix. Numerous studies have concentrated on the compressive behaviour of cylindrical composite tubes. Khalili et al.

[21] observed that nano-silica improved compressive modulus and axial load capacity. Movahedi et al. [22] documented enhanced stability and decreased buckling deformation in hybrid composite shells. Panigrahi et al. [23] emphasized the influence of filler dispersion quality on compressive failure patterns. Bhatnagar et al. [24] highlighted that uniform nanoparticle dispersion substantially enhances structural integrity, whereas Venugopal et al. [25] demonstrated that filler-modified epoxy matrices result in superior compressive strength in filament-wound cylinders.

The literature study indicates that the mechanical properties of GFRP composites are considerably affected by factors like fiber architecture, shell shape, manufacturing methods, and particularly the inclusion of fillers. Previous studies consistently demonstrate that nanofillers, such as fumed silica, are essential for improving flexural rigidity, compressive stability, and overall structural performance. Nevertheless, the majority of researchers concurred that high filler loading results in particle agglomeration, matrix discontinuities, and premature failure. This directly underpins the rationale of the current study, which examines the impact of different Aerosil-200 nanofiller concentrations (0–4 wt.%) on the flexural and compressive properties of GFRP laminates and cylindrical shells. This study seeks to identify the ideal nanofiller concentration that enhances mechanical performance while maintaining structural integrity by combining ideas from previous research with current experimental findings.

2. Methodology

2.1 Materials and Methods

The materials utilized in this study were meticulously chosen to guarantee superior mechanical performance and structural integrity of the produced composite laminates. Bidirectional E-glass fiber functioned as the principal reinforcement owing to its superior tensile strength, dimensional stability, and compatibility with epoxy systems. This woven roving fabric offers consistent mechanical properties in two perpendicular directions, rendering it suitable for load-bearing composite structures. The matrix system comprised Araldite LY 556 epoxy resin, a medium-viscosity Bisphenol-A formulation recognized for its robust adhesive properties, chemical resistance, and processing convenience. The resin was cured using Aradur HY 951, a low-viscosity aliphatic amine hardener that provides exceptional tensile and impact strength, as well as outstanding bonding capabilities. The resin–hardener system collectively creates a robust and inflexible polymer matrix that efficiently transmits stresses to the fiber reinforcement.

To improve the mechanical properties of the composites, Aerosil 200 fumed silica was added as a nanofiller. This ultrafine silica powder enhances resin viscosity, prevents sedimentation, and improves matrix homogeneity by serving as an anti-caking and thickening agent. The incorporation of nanofiller enhances the fiber - matrix interface, leading to better flexural and compressive properties. Accurate formulations were created by meticulously weighing all components, and the epoxy–hardener blend was kept at a 20:1 weight ratio to guarantee consistent curing. Fumed silica was incorporated in different proportions of 0%, 1%, 2%, 3%, and 4% by weight to create five distinct composite specimens. This systematic variation facilitated a thorough assessment of how nanofiller concentration affects the structural, mechanical, and failure properties of the GFRP laminates.

2.2. Hand Layup Technique

The hand lay-up technique is a commonly used fabrication method for creating composite laminates, appreciated for its straightforwardness, design versatility, and economical

advantages. The initial step involves preparing the mould surface by applying an appropriate release agent to ensure that there is no adhesion between the laminate and the mould. A mandrel made from plaster of Paris serves as the foundational form for cylindrical components. Bidirectional E-glass fibre layers are meticulously arranged by hand over the mandrel to attain the specified reinforcement orientation. The mixture of epoxy resin and hardener, adjusted with different amounts of Aerosil 200 nanofiller, is consistently applied across the fibre layers with brushes and rollers, guaranteeing thorough wetting and penetration of the resin into the fibre network. Every layer is meticulously consolidated to eliminate trapped air bubbles and improve the bonding between the fibre and matrix.

The lamination process proceeds by sequentially layering fibres and applying resin until the desired thickness is reached. In the process of laying, rollers play a crucial role in compacting the laminate and ensuring an even distribution of resin, which effectively minimises void content and enhances mechanical consistency. After achieving the desired lay-up, the composite is permitted to cure undisturbed at room temperature. The curing process solidifies the resin matrix, effectively bonding the reinforcement layers into a rigid structure. Upon complete curing, the cylindrical laminate is carefully removed from the mandrel and precisely trimmed to the specified dimensions. The hand lay-up process, though manual, provides meticulous control over fibre placement and filler distribution, rendering it especially appropriate for experimental investigations that necessitate tailored laminate configurations.

To guarantee the repeatability of the hand-layup specimens, all manufacturing procedures were standardized and executed under meticulously regulated conditions. Identical resin, hardener, glass fiber batch, and Aerosil-200 nanofiller were employed in all experiments to eliminate material variability. The processing parameters, including the resin–hardener ratio (20:1), nanofiller mixing duration, fiber orientation, lay-up sequence, and curing duration, were standardized across all specimen groups. For each nanofiller concentration, three replicate specimens were produced and evaluated, revealing a variance in flexural and compressive strengths of only 5–7%, thereby affirming the reliable repeatability of hand-layup composites. SEM analysis of representative samples confirmed that microstructural characteristics, including void content, fiber–matrix adhesion, and fracture morphology, were consistent across replicates, indicating that the fabrication process yielded uniform and reproducible composite specimens appropriate for comparative mechanical assessment. Figure 1 illustrates the hand layup procedure for a thin cylinder.



Fig. 1. Hand layup process of thin cylinder.

3. Experimentation

3.1 Flexural Test of laminated specimens

The flexural strength of a glass-epoxy cylindrical shell is an essential mechanical parameter that indicates its capacity to withstand deformation under bending forces. The flexural strength of cylindrical shells is influenced by various factors, including the type of reinforcement, fibre orientation, resin content, filler material, and production procedures. Glass fibres serve as the reinforcement, delivering the principal load-bearing capacity, whereas the epoxy resin matrix facilitates effective bonding and load transfer among the fibres. The orientations of the woven fibres are utilised to improve mechanical performance, particularly under bending forces. The evaluation of flexural strength is often performed using a three-point bending test, in which a consistent force is applied until the specimen fractures or fails. The cylindrical form of the shell presents complexity, including hoop stresses, that must be considered during testing. Factors like fibre volume fraction, shell thickness, and loading conditions substantially affect flexural strength. Optimal fibre orientation and adequate curing of the epoxy matrix are crucial for attaining optimal strength. The flexural strength of glass-epoxy cylindrical shells is a critical factor for their dependability and efficacy in structural applications.

The flexural test was performed on laminated specimens reinforced with different weight percentages of Aerosil 200 filler (1%, 2%, 3%, and 4%) to assess their mechanical properties. This test evaluates the material's capacity to withstand bending pressures, providing essential information regarding its flexural strength. The specimens were created by a regulated lamination procedure, guaranteeing consistent distribution of fillers inside the matrix. The fillers were integrated to improve mechanical qualities, including stiffness and load-bearing capacity, while preserving the structural integrity of the laminates. Each specimen underwent a three-point bending test utilising a universal testing machine, in accordance with ASTM D790 criteria. Figure 2 illustrates the laminated glass fibre specimens and the bending of these laminated specimens.

a)



b)

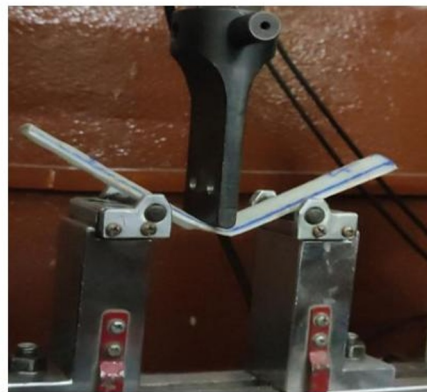


Fig. 2. Images of a laminated glass fiber specimens b. Bending on laminated specimens.

3.2 Compression Test on Cylindrical Shell

Compression testing is an essential technique for assessing the mechanical properties of composite materials, including cylindrical glass epoxy shells, which are extensively utilised in aerospace, automotive, and structural applications owing to their superior strength-to-weight ratio. The examination entails exerting a regulated compressive force on the shell to

assess its load-bearing capacity, deformation properties, and failure processes. Glass epoxy shells, composed of glass fibres embedded in an epoxy resin matrix, demonstrate a complicated failure pattern under compression, affected by fibre orientation, shell shape, and loading conditions.

The cylindrical shell is meticulously fabricated to exact specifications and positioned within a testing apparatus to guarantee even load distribution. A universal testing machine (UTM) with a capacity of 600 kN is utilised, fitted with compression platens and strain measurement instruments. With increasing load, the shell may undergo elastic deformation, subsequently transitioning to plastic deformation and ultimately failing owing to buckling, delamination, or fibre fracture. The outcomes of compression tests encompass the maximum compressive strength, modulus of elasticity, and strain at failure. These metrics offer insights into the material's behaviour and assist in developing components to endure operational loads. Variables like shell thickness, aspect ratio, filler content, and ambient factors such as temperature and humidity substantially influence the test results. Figure 3 illustrates the incremental failure of the composite shell during the compression test.



Fig. 3. Progressive failure of composite shell during compression test.

4. Results and Discussions

4.1 Flexural Test

A slender laminate (200 mm × 30 mm × 2 mm) was subjected to bending until failure to determine the ultimate load, flexural strength (σ_f), and the fracture point (load and displacement at which the specimen fails). A unified graphic displays all curves (0–4% Aerosil), illustrating a fast ascent to a peak, succeeded by post-peak relaxation and fracture at 20 mm. The consistent rise in σ_f from 0–3% demonstrates that minimal quantities of Aerosil (fumed silica) effectively enhance the matrix's strength. Nanoparticles can inhibit crack formation and propagation (micro crack pinning, crack deflection) and enhance stress transfer at the matrix/fiber or matrix/matrix interfaces. The optimal concentration of approximately 3% is characteristic of nanoparticle-reinforced systems; beyond a critical loading result in agglomeration and inadequate wetting, which generates stress concentrators

that diminish effective strength, as evidenced at 4%. The observed initial slope is greatest at 3%, indicating a more rigid bending reaction. The 1–2% and 4% mixtures exhibit reduced apparent stiffness compared to the plain laminate, indicating that the effects of dispersion quality and resin viscosity prevail at these concentrations. The elevated viscosity resulting from the addition of aerosil may impede impregnation and create micro voids, both of which diminish stiffness if the dispersion is not ideal.

The 3% laminate attains the highest peak load and the largest area under the curve, signifying the optimal combination of strength and energy absorption among the evaluated levels. The 4% laminate demonstrates a significantly reduced residual load and the least work to fracture, aligning with embrittlement due to particle agglomerates and flaws that facilitate premature microcracking and accelerated softening beyond the peak threshold. The well-structured laminate maintains a considerable post-peak load (402 N at fracture) and a substantial work to fracture. This indicates that, despite its maximum strength being inferior to the 3% system, it yet demonstrates steady post-peak softening. In this laminate and testing configuration, a 3% aerosil loading is deemed ideal, since it concurrently enhances flexural strength, stiffness, and work to fracture. To get optimal bending strength and a resilient post-peak reaction, aim for 3%. Should process restrictions necessitate elevated filler levels (e.g., viscosity regulation, flame retardancy), anticipate diminished peak strength and toughness unless dispersion is enhanced (e.g., surface-treated silica, optimised mixing/degassing). Aerosil nanofiller enhances flexural performance by up to 3%, resulting in the laminate attaining its maximum flexural strength (590.6 N/mm²), peak load (853 N), and greatest effort to fracture. At 4%, characteristics deteriorate - likely attributable to particle agglomeration and defect formation—highlighting the significance of dispersion quality and an appropriate filler threshold for enhancing flexural strength and toughness. Figure 4 illustrates the load versus displacement of several nanofillers.

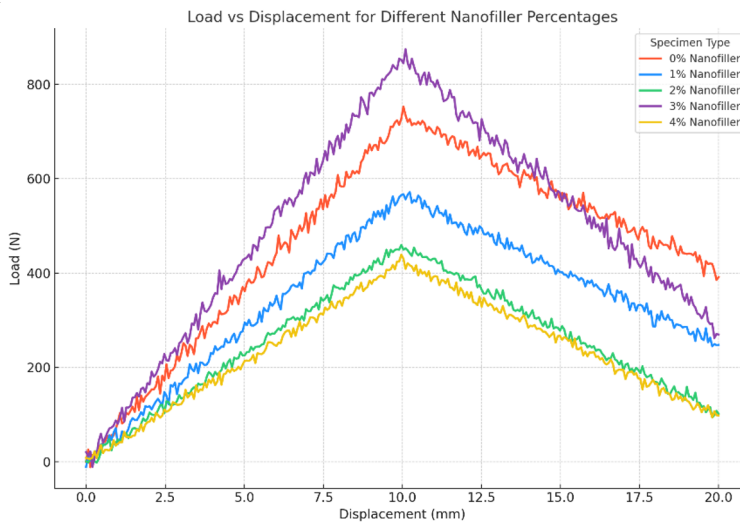


Fig. 4. Load vs displacement of different nanofiller.

4.2 Compression Test

The compression test performed on hollow cylindrical GFRP shells reinforced with different Aerosil-200 nanofiller concentrations demonstrated a distinct and incremental improvement in compressive load-bearing capability up to 3% nanofiller. The specimen devoid of nanofiller demonstrated a peak load of 29.820 kN, a CHT of 3.94 mm, and a compressive strength of 87.889 N/mm², establishing the baseline for comparison. The incorporation of

nanofiller resulted in a moderate although consistent enhancement, yielding compressive strengths of 90.984 N/mm² for the 1% specimens and 96.595 N/mm² for the 2% specimens. The enhancements are ascribed to improved stress transfer within the matrix and augmented microstructural stability, as Aerosil nanoparticles refine the epoxy network and diminish micro-voids. The elevated CHT value at 1% filler (8.83 mm) signifies increased deformation prior to peak load, implying enhanced ductility and postponed instability under axial compression. A notable change in behaviour transpires at 3% Aerosil, where the cylindrical shell exhibits a substantially elevated peak load of 58.230 kN and a compressive strength of 157.663 N/mm², indicating an approximate 79% enhancement compared to the unfilled specimen. This significant enhancement underscores the ideal interaction between the nanofiller and the epoxy matrix at this concentration: the nanoparticles proficiently impede crack initiation, fortify the fiber-matrix interface, and augment resistance to local buckling modes that usually dominate thin-walled composite shells. The 3% specimen has a moderate CHT of 6.10 mm, indicating a harmonious blend of rigidity and regulated deformation before collapse. The significant increase in compressive capacity at this filler level indicates that the shell derives optimal advantages when the silica nanoparticles are thoroughly disseminated and completely integrated into the resin microstructure. The observed fluctuations in CHT are significantly associated with the advancement of microstructural degradation in the composite shells. Elevated CHT values (evident in the 1% and 2% nanofiller specimens) signify that the shell experiences a greater degree of controlled axial deformation prior to instability, implying postponed microcrack onset and enhanced matrix continuity. At 3% nanofiller content, the CHT remains moderate, indicating an appropriately reinforced microstructure that impedes crack propagation by mechanisms such as crack deflection, enhanced bonding, and localized energy dissipation. The reduced CHT reported at 4% nanofiller aligns with early microstructural degradation due to filler agglomeration, void creation, and resin discontinuities. These imperfections function as stress concentrators, expediting fracture propagation and leading to premature failure of the shell. Consequently, CHT functions as a precise gauge of the rate and degree of microstructural damage development, where elevated tolerance values signify postponed damage propagation, while diminished values denote the early emergence of matrix cracking, debonding, and instability.

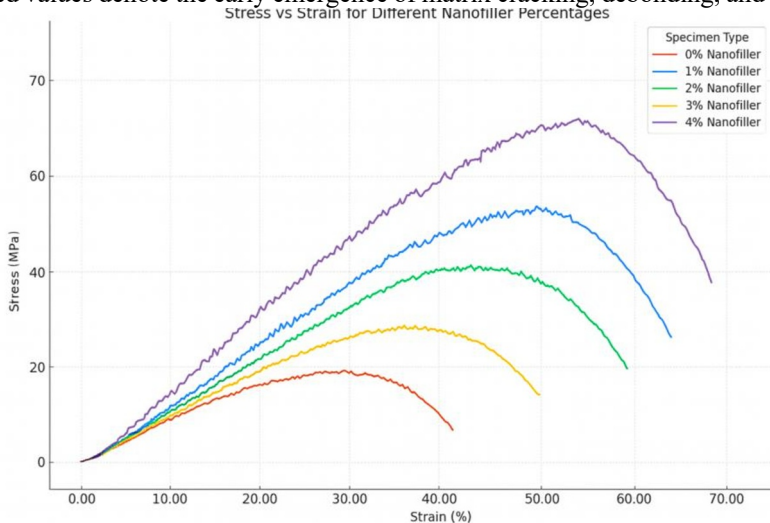


Fig. 5. Stress vs strain of different nanofiller.

Figure 5 illustrates the relationship between stress and strain for various nanofillers. Nonetheless, an additional increase of the nanofiller to 4% leads to a decrease in performance, as indicated by a lower peak load of 40.980 kN and a compressive strength of 116.34 N/mm².

This reduction aligns with the common behaviour observed in over-filled nanocomposites, where an excess of Aerosil results in particle agglomeration, thickening of the resin, and inadequate wet-out of the fibres, leading to stress concentrations that hasten failure. The reduced CHT at 4% (3.75 mm) suggests an early onset of instability or brittle behaviour. The findings indicate that the compressive behaviour of the cylindrical composite shell is notably enhanced with the incorporation of Aerosil nanofiller, but this improvement is limited to an optimal threshold of 3%. Beyond this point, the structural integrity declines as a result of defects induced by the filler. The results are consistent with established theories in the field and demonstrate that a concentration of 3% Aerosil-200 is optimal for enhancing compressive strength, stiffness, and deformation capacity in thin-walled composite cylinders.

5. Morphological Analysis

The fracture morphology of the composite specimens was analysed via Scanning Electron Microscopy (SEM) to elucidate the microstructural mechanisms influencing the flexural and compressive failure of GFRP composites supplemented with different quantities of Aerosil-200 nanofiller. The SEM pictures demonstrate distinct indications of matrix cracking, fiber–matrix interfacial debonding, void formation, fibre pullout, and shear deformation. The morphological characteristics corroborate the mechanical results and offer a more profound understanding of the impact of nanofiller content on microstructural integrity and failure progression. The SEM image (a) displays significant matrix cracking, marked by acute, brittle fracture lines and crater-like indentations. These characteristics suggest that failure mostly originated within the epoxy matrix as a result of localised stress concentrations. The crater formations indicate micro-void coalescence succeeded by fast crack propagation, a phenomenon typically linked to inadequate ductility of the polymer matrix or suboptimal filler dispersion. The stratified, flake-like resin architecture indicates insufficient stress transfer among matrix layers, resulting in early failure. This shape is characteristic of composites with reduced nanofiller content or areas where the matrix predominantly bears the load. The fracture depicted in figure (a) indicates a matrix-dominated brittle failure mechanism.

Image (d) displays distinct voids that function as stress concentration locations and serve as loci for crack initiation. These voids presumably originated during manufacturing due to retained air, insufficient degassing, or localized filler aggregation. The fracture surface reveals crack initiation zones, indicated by areas where the matrix shows abrupt tearing in conjunction with fiber rupture. The presence of voids, microcracks, and resin discontinuities indicates that structural integrity is weakened in areas with non-uniform nanofiller dispersion. This behaviour aligns with the mechanical observations for elevated filler percentages (e.g., 4%), where excessive Aerosil concentration results in brittleness due to agglomeration. Consequently, SEM image (d) underscores microstructural vulnerabilities caused by flaws that hasten failure. Figure 6 illustrates the SEM images depicting a) matrix cracking and crater formation on the fracture surface, and b) fiber pullout and shear hackle creation in the banana fiber composite. c) Edge chipping and fiber pullout signifying interfacial debonding d) Void formation and fracture initiating regions within the composite microstructure.

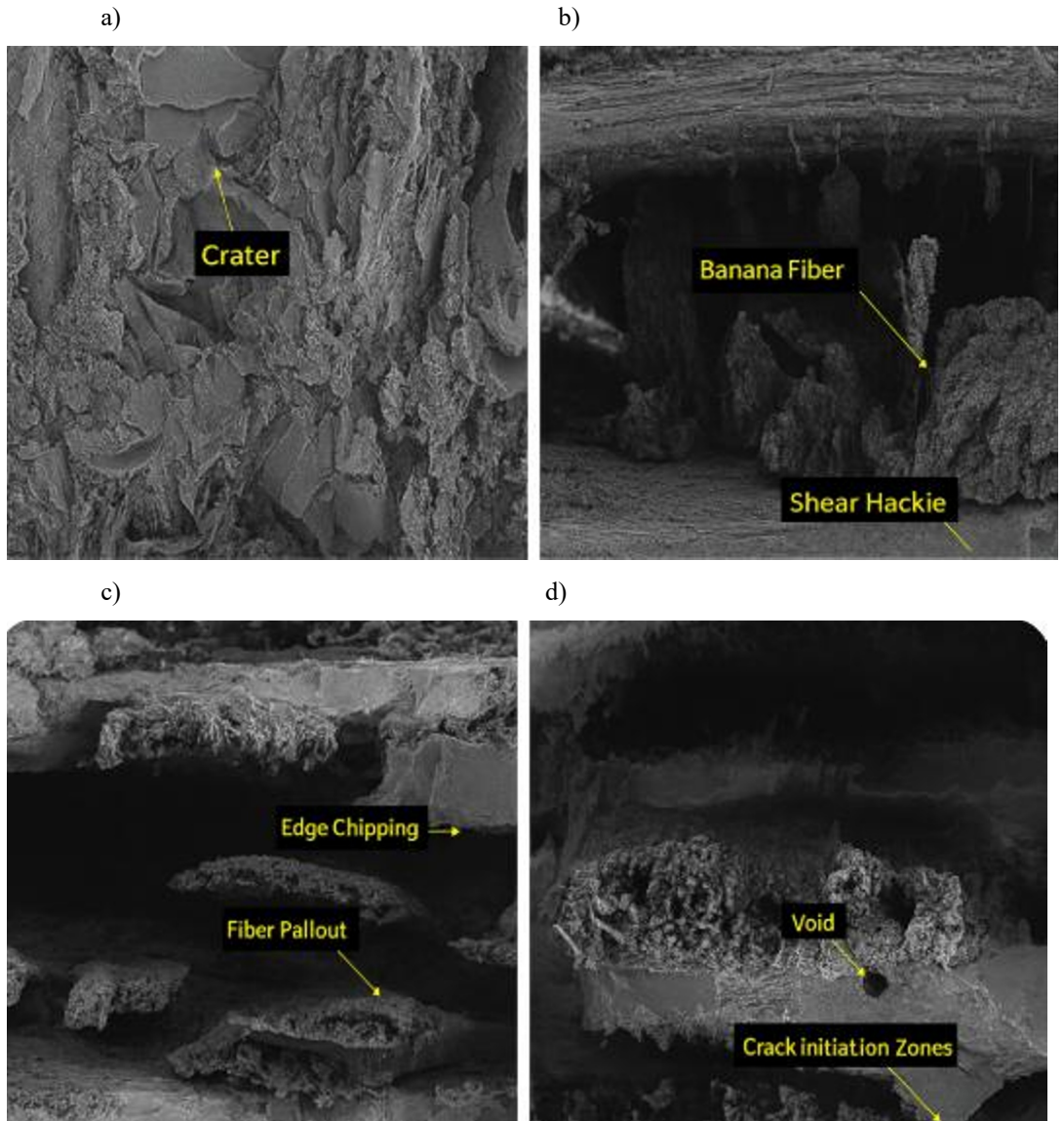


Fig. 6. SEM Images of a) matrix cracking and crater formation in the fracture surface b) fiber pullout and shear hackle formation in banana fiber composite c) edge chipping and fiber pullout indicating interfacial debonding d) void formation and crack initiation zones in composite microstructure.

Image (b) reveals significant fibre pullout voids and exposed fibre surfaces, signifying inadequate fiber–matrix adhesion. The existence of banana fibres indicates insufficient resin penetration around the fibre surfaces, perhaps due to elevated mixture viscosity at certain filler concentrations. The extremely directed shear hackles - delicate, ridge-like formations aligned with the crack path - indicate that the crack advanced under a combination of shear and tensile stresses. The prominent fibre pullout zones indicate that rather than breaking,

fibres disengaged from the matrix, absorbing energy and facilitating a certain level of ductile behaviour. The shear hackle patterns observed in SEM image (b) further validate the occurrence of mixed-mode crack propagation inside the composite microstructure. Hackles are formed when a propagating crack encounters areas of interfacial debonding or irregular stress distribution, causing the crack to diverge from a linear Mode-I trajectory and advance along inclined shear planes. The development of these ridge-like hackle marks signifies that the crack front underwent multiple redirections while progressing around partially debonded fibers, resin-rich areas, and localized stress concentrations. Thus, the observed shear hackles indicate that fracture in this area was controlled by shear-dominated crack propagation, consistent with the fiber pullout characteristics and the mechanical loading circumstances that initiated local shear stresses in the composite.

This image illustrates a mixed-mode failure, wherein shear forces, interfacial debonding, and insufficient fibre embedding jointly induce the fracture process. The SEM image (c) demonstrates considerable edge chipping and stepped fracture layers, signifying initial delamination at the laminate interfaces. The consistent observation of fibre pullout verifies that debonding at the fiber–matrix interface is a primary failure mechanism in this area. The irregular microstructure and numerous fracture planes indicate that localised resin-deficient areas contributed to the onset of microcracks, which subsequently spread along the fibre layers. Progressive delamination is apparent from the stratified morphology, indicative of interlaminar shear failure. The identified microstructural flaws suggest inadequate matrix impregnation or filler agglomeration, which diminish load transfer efficiency. Consequently, image (c) illustrates failure predominantly caused by interfacial debonding and delamination.

6. Conclusion

The study reveals significant trends in the flexural and compressive strength of laminated specimens enhanced with varying percentages of Aerosil nanofiller. The experimental results indicate a gradual improvement in the flexural strength of the laminated specimens as the Aerosil nanofiller concentration increases from 0% to 3%. Specifically, the flexural strength values rise consistently from 399.9 N/mm² (0%), 459.41 N/mm² (1%), 535.25 N/mm² (2%), and peak at 590.59 N/mm² (3%). However, beyond 3%, at a 4% nanofiller concentration, the flexural strength declines significantly to 345.5 N/mm², suggesting a potential over-saturation or negative interaction of the filler at higher levels. Similarly, compressive strength trends exhibit a steady increase with nanofiller content from 0% to 3%. At 3% nanofiller, the compressive strength peaks at 157.663 N/mm², corresponding to a peak load of 58.230 kN and a compressive heat transfer (CHT) of 6.10 mm. However, a further increase to 4% nanofiller results in a reduction of compressive strength to 116.34 N/mm², with a peak load of 40.98 kN and CHT of 3.75 mm. This decline highlights the diminishing mechanical benefits of higher nanofiller concentrations. The findings underscore that incorporating Aerosil-200 nanofiller enhances the mechanical properties of the specimens up to an optimal threshold of 3%.

Beyond this limit, excessive nanofiller content adversely affects both flexural and compressive strengths, likely due to issues such as filler agglomeration or structural inefficiencies in the composite matrix. This study recommends two enhancements to increase the mechanical performance of Aerosil-reinforced GFRP composites. The application of sophisticated nanofiller dispersion methods—such as ultrasonic homogenization, high-shear mechanical stirring, or surface-treated silica—can markedly diminish agglomeration and void formation, thereby enhancing interfacial adhesion and postponing microcrack start. Secondly, the integration of hybrid toughening agents such as graphene nanoplatelets, nanoclay, or core-shell rubber particles could yield synergistic benefits that enhance both peak load capacity and post-peak deformation behaviour. These methodologies tackle the microstructural constraints seen at elevated filler concentrations and provide distinct avenues

for enhancing composite performance in future research. These results provide valuable insights for optimizing the formulation of nanocomposite materials to achieve superior mechanical performance.

Declaration of Interest

The author(s) have disclosed no conflicts of interest.

Acknowledgements

Not Applicable

Data Availability Statement

This study does not develop nor examines any new data

Ethics Statement

This material was created by the author alone, hasn't been published anywhere else, and isn't currently being considered for publishing anywhere. It fully and properly reflects the study and analysis of the author or authors.

Funding

Funding is not available to report.

References

1. M.C. Ray, Buckling and postbuckling characteristics of composite cylindrical shells M.C. Ray, Buckling and postbuckling characteristics of composite cylindrical shells under axial compression. *Composite Structures* 74(3) (2006).
2. G. Ashwin Prabhu, G. Karuppaswamy, J.M. Babu, K. Shekar, V.S. Vishnu Aher, S. Prathap Singh, R. Rangaraja, F. Antony Leo, K. Deepak, S. Aswin, Development and assessment of mechanical characteristics in sisal–glass fiber reinforced epoxy composites. *Journal of Polymer and Composites* 13(5), 708–719 (2025).
3. R. Kumar, S. Singh, Mechanical behaviour of glass fiber epoxy composites with nano-SiO₂ particles. *Materials Today: Proceedings* 18 (2019).
4. A. Verma, R. Sharma, Effect of nanoclay on flexural and impact properties of GFRP composites. *Polymer Composites* 42(1) (2021).
5. G. Ashwin Prabhu, R. Rajesh Sudhakar, R. Sathishkumar, G.M. Lionus Leo, B. Aarsath Crisple, A.H. Abdul Rahman, Dynamic mechanical analysis of carbon fiber reinforced polymer composites. *Journal of Polymer and Composites* 13(5), 386–393 (2025).
6. S.S. Mirjalili, H.R. Bahrami, Mechanical performance of CNT-reinforced epoxy composites. *Journal of Reinforced Plastics and Composites* 34 (2015).
7. S. Chandra, P. Rao, Axial compression failure of glass/epoxy tubes. *Composite Structures* 132 (2015).
8. M.K. Gupta, V. Chaudhary, Hybrid natural fiber/silica–epoxy composites: Mechanical studies. *Journal of Materials Research* 35 (2020).
9. W.Y. Li, L. Chen, Influence of graphene oxide on flexural strength of epoxy laminates. *Journal of Applied Polymer Science* 137 (2020).
10. K.P. Shanmugam, R. Alagar, Study of silica–epoxy nanocomposites. *Materials Research Express* 5 (2018).
11. S. Alavi, A. Ashrafi, Compression behaviour of filament-wound composite cylinders. *Thin-Walled Structures* 145 (2019).

12. J. Heidari-Rarani, M. Shokrieh, Flexural stiffness and failure analysis of GFRP laminates. *Composite Part B: Engineering* 62 (2014).
13. G. Ashwin Prabhu, R. Selvam, K. Muninathan, J. Janarthanam Vijayanand, P. Premkumar, A. Ruskin Bruce, D. Sakthivel, T. Balasubramanian, J. Jeyasuriya, M. Mohamed Rashath, Mechanical characterization of hybrid basalt fiber composites with silicon carbide fillers. *Journal of Polymer and Composites* 13(4), 582–593 (2025).
14. P.K. Sarker, T. Hossain, Mechanical enhancement in silica-filled epoxy nanocomposites. *Journal of Polymer Engineering* 40 (2020).
15. K. Patel, S. Patel, Mechanical and morphological properties of silica nanoparticle reinforced epoxy resin. *Journal of Nanostructures* 10 (2020).
16. G. Ashwin Prabhu, S. Raja, S. Murugapoopathi, M. Santhosh, R. Aswanth Singh, J. Dhanush, Enhancing mechanical and thermal properties of glass fiber-reinforced epoxy composites with silicon carbide additives. *Journal of Polymer and Composites* 13(4), 69–77 (2025).
17. A. Dasari, J. Misra, Effect of fiber orientation on bending behaviour of GFRP laminates. *Materials and Design* 92 (2016).
18. O. Faruk, M. Sain, Properties of nano-filler modified epoxy reinforced laminates. *Journal of Composite Materials* 49 (2015).
19. G. Ashwin Prabhu, E. Eanest Jebasingh, V.S. Vishnu Aher, I. Ameeth Basha, A. Sargunraj, V. Gopal, M. Pranav Raj, N. Naveen Samuel, Comprehensive experimental analysis of the mechanical properties and enhancements of natural fiber composites. *Journal of Polymer and Composites* 13(4), 45–53 (2025).
20. A.R. Siddiquee, P. Tiwary, Mechanical characterization of E-glass/epoxy cylindrical tubes. *Materials Science and Engineering* 577 (2019).
21. G. Ashwin Prabhu, G. Magudeeswaran, S. Murugapoopathi, M. Santhosh, K. Rahul, S. Thejeshwaran, Evaluating the durability and environmental sustainability of hybrid natural–synthetic fiber composites. *Journal of Polymer and Composites* 13(4), 93–102 (2025).
22. A. Rahman, Q. Li, Axial crushing performance of fiber-reinforced tubes. *Composite Structures* 220 (2019).
23. P.S. Suresh, K. Kanny, Impact and flexural behaviour of silica–epoxy nanocomposites. *Composites Communications* 12 (2019).
24. V.G. Reddy, S. Chandra, Experimental analysis of silica-filled GFRP composite laminates. *Materials Today: Proceedings* 49 (2022).
25. M. Santhosh, D. Priya Matharasi, G. Ashwin Prabhu, M. Siva, M. Arivarasu, R. Athithyan, Mechanical analysis and advanced manufacturing of eco-friendly groundnut shell powder reinforced epoxy composites. *Journal of Polymer and Composites* 13(5), 174–185 (2025).